Recent results on baryon spectroscopy at ELSA and MAMI

QCHSC 2024

Farah Afzal for the CBELSA/TAPS and A2 collaboration

21.08.2024

University of Bonn

Light baryon spectroscopy

Light baryon excitation spectrum

UNIVERSITÄT BONN

Bound states of strong QCD are not yet understood!

Quark model vs. experimental data

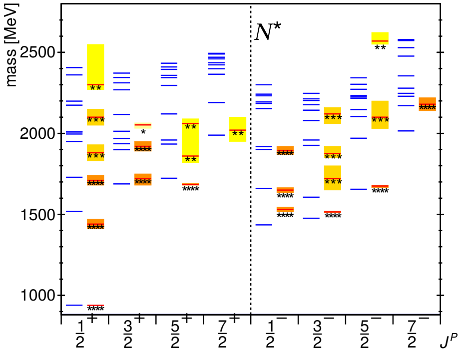

[U. Loering, B.C. Metsch, H.R. Petry, EPJA 10 (2001) 395-446]

Lattice QCD

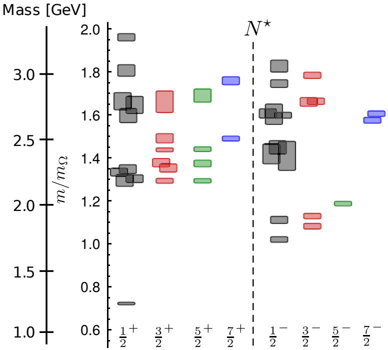

[R. G. Edwards et al., Phys. Rev. D 84 (2011) 074508]

- Discrepancy between theory and experiment: missing resonances, systematics of spectrum

Light baryon excitation spectrum

Bound states of strong QCD are not yet understood!

Quark model vs. experimental data

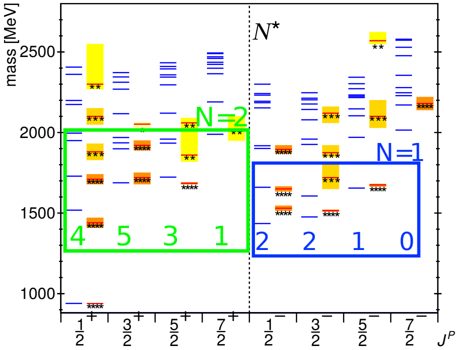

[U. Loering, B.C. Metsch, H.R. Petry, EPJA 10 (2001) 395-446]

Lattice QCD

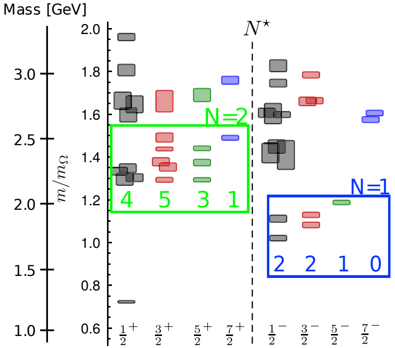

[R. G. Edwards et al., Phys. Rev. D 84 (2011) 074508]

- Discrepancy between theory and experiment: missing resonances, systematics of spectrum
- most resonances observed in elastic πN scattering until 2010 $\rightarrow$ experimental bias?

Worldwide effort to get high precision data (ELSA, MAMI, JLab, SPring-8, ...)

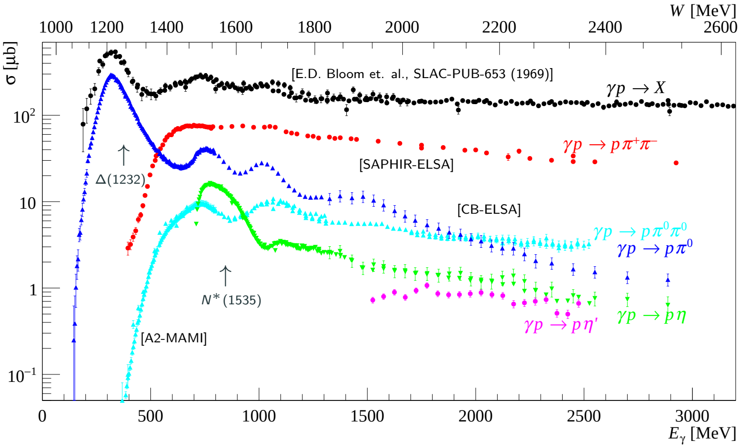

[A. Thiel, F. Afzal, Y. Wunderlich, Prog. Part. Nucl. Phys. 125 (2022) 103949]

- Photoproduction reactions are an excellent tool to probe excitation spectra!
- Resonances contribute with different strength to distinct channels
- How can we disentangle contributing resonances?

UNIVERSITÄT BONN

Polarization observables in the 2-body kinematic system for the photoproduction of a pseudoscalar meson

Photon polarization		Target polarization			Recoil nucleon polarization			Target and recoil polarizations			
		X	Y	Z(beam)	X'	Y'	Z'	X' X	X' Z	Z' X	Z' Z
unpolarized	σ	-	T	-	-	P	-	$T_{x'}$	$L_{x'}$	$T_{z'}$	$L_{z'}$
linear	$-\Sigma$	H	(-P)	-G	$O_{x'}$	(-T)	$O_{z'}$	$(-L_{z'})$	$(T_{z'})$	$(L_{x'})$	$(-T_{x'})$
circular	-	F	-	-E	$C_{x'}$	-	$C_{z'}$	-	-	-	-

σ, Σ, T, P + 4 double pol. observables needed for a unique solution

[W. Chiang and F. Tabakin, Phys. Rev., C55 (1997) 2054-2066]

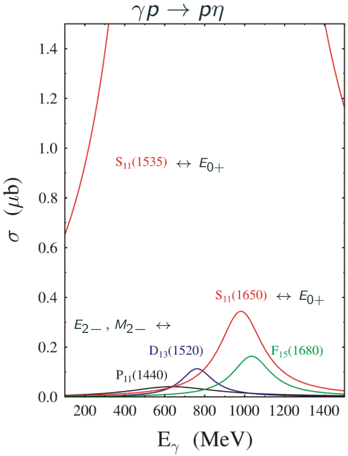

Polarization observables in the 2-body kinematic system for the photoproduction of a pseudoscalar meson

Photon polarization		Target polarization			Recoil nucleon polarization			Target and recoil polarizations			
		X	Y	Z(beam)	X'	Y'	Z'	X' X	X' Z	Z' X	Z' Z
unpolarized	σ	-	T	-	-	P	-	$T_{x'}$	$L_{x'}$	$T_{z'}$	$L_{z'}$
linear	$-\Sigma$	H	(-P)	-G	$O_{x'}$	(-T)	$O_{z'}$	($-L_{z'}$)	($T_{z'}$)	($L_{x'}$)	($-T_{x'}$)
circular	-	F	-	-E	$C_{x'}$	-	$C_{z'}$	-	-	-	-

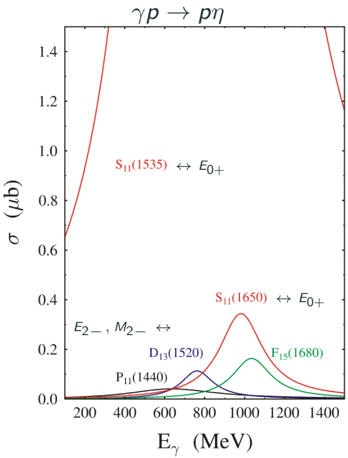

$\sigma, \Sigma, T, P + 4$ double pol. observables needed for a unique solution

[W. Chiang and F. Tabakin, Phys. Rev., C55 (1997) 2054-2066]

$$\sigma \sim |E_{0+}|^2 + |E_{1+}|^2 + |M_{1+}|^2 + |M_{1-}|^2 + \ldots$$

$$\Sigma \sim \underbrace{-2E_{0+}^* E_{2+} + 2E_{0+}^* E_{2-} - 2E_{0+}^* M_{2+} + 2E_{0+}^* M_{2-}}_{< S, D >} + \ldots$$

$\rightarrow$Polarization observables are sensitive to interference terms!

$\rightarrow$Interferences with the dominant S-wave (E_{0+}) important in η photoproduction!

Development of database

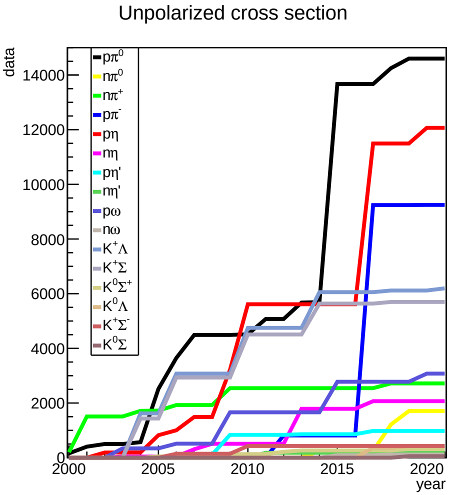

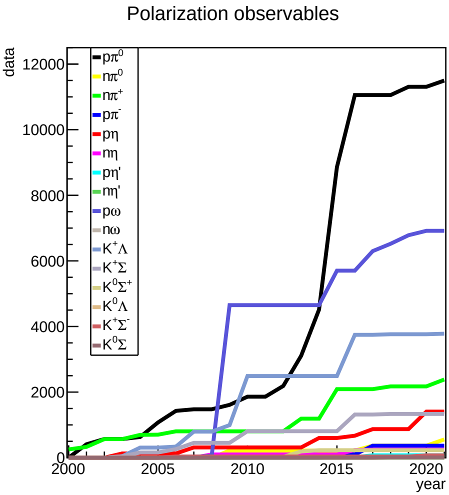

[A. Thiel, F. Afzal, Y. Wunderlich, Prog. Part. Nucl. Phys. 125 (2022) 103949]

Experimental facilities at MAMI and ELSA

Experimental facilities at MAMI and ELSA

A2@MAMI

- Electron beam: 0.18 GeV - 1.6 GeV
- Continuous beam
- Crystal Ball (NaI) + TAPS (BaF_2 & $PbWO_4$)
- PID, MWPCs, Vetos

CBELSA/TAPS@ELSA:

- Electron beam: 0.6 GeV - 3.2 GeV
- Quasi-continuous beam
- Crystal Barrel (CsI) + MiniTAPS (BaF_2)
- Inner detector, Vetos

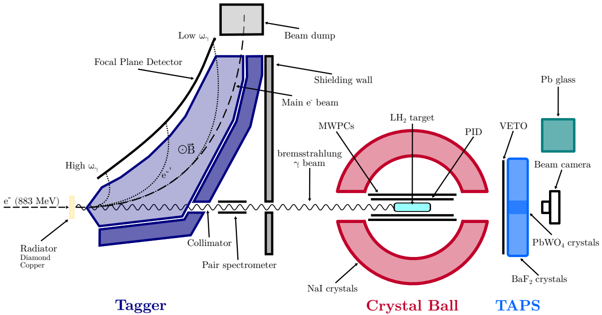

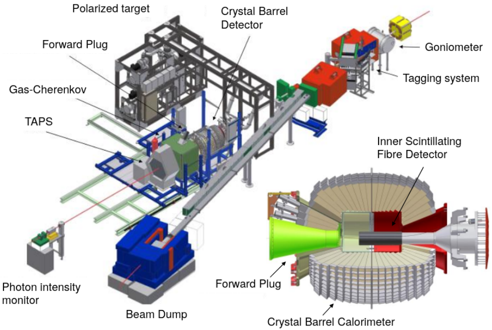

Linearly polarized photons

- diamond radiator needed
- coherent bremsstrahlung
- coherent edges at: e.g. 1200 MeV

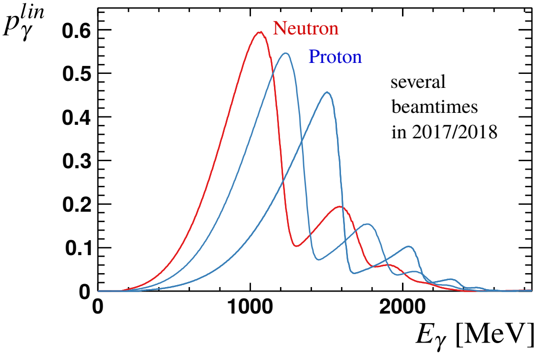

Circularly polarized photons

- long. polarized electrons needed
- helicity transfer to photons
- Mott/Møller measurement: $p_e \approx 75\% - 78\%$

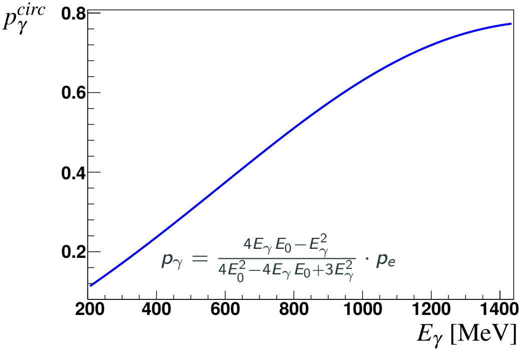

- Collaboration between Bonn (H. Dutz), Mainz (A. Thomas) and Bochum (G. Reicherz)
- polarization via Dynamic Nuclear Polarization DNP
- maximal pol. degree: $p_T \approx 89\%$
- relaxation times: 1800 h - 2000 h

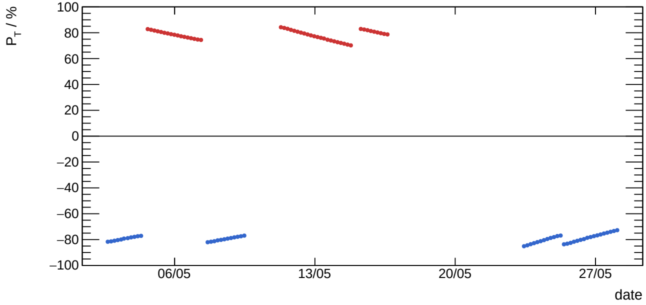

Measurements off protons ($\gamma p \rightarrow p\pi^0$)

$\gamma p \rightarrow p\pi^0$: Measurement of cross sections (A2)

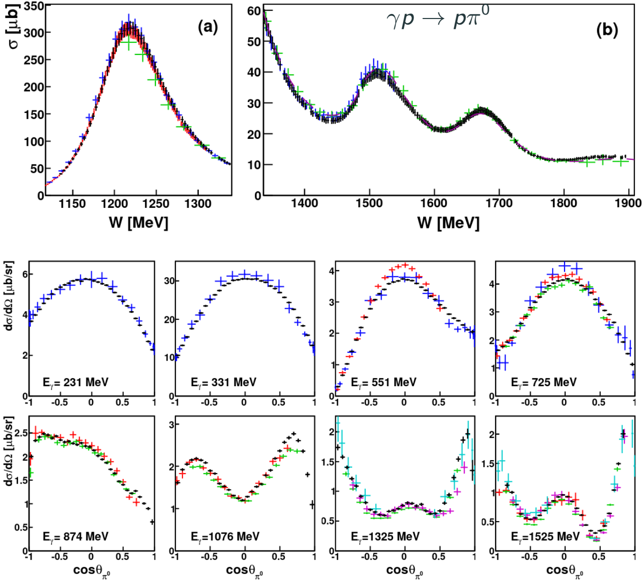

+ other MAMI data   + GRAAL   + CLAS   + CB-ELSA   + CBELSA/TAPS

P. Adlarson et al., Phys. Rev. C92.2 (2015), p. 024617

+ other MAMI data, + other MAMI data, + CB-ELSA

- fine energy binning
- full angular coverage
- increases existing data by 47%

Elliptically polarized photons (long. pol. electrons + diamond) and longitudinally polarized target:

$$\frac{d\sigma}{d\Omega}(\theta,\phi) = \frac{d\sigma}{d\Omega}_0(\theta)\left[1 - P_{lin}\boldsymbol{\Sigma}\cos(2(\alpha-\phi)) - P_z\left(-P_{lin}\mathbf{G}\sin(2(\alpha-\phi)) + P_{circ}\mathbf{E}\right)\right]$$

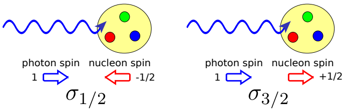

Helicity asymmetry: $E = \frac{\sigma_{1/2}-\sigma_{3/2}}{\sigma_{1/2}+\sigma_{3/2}}$

△ M. Gottschall et al. (CBELSA/TAPS, $p\pi^0$), Eur. Phys. J. A 57.1 (2021), p. 40

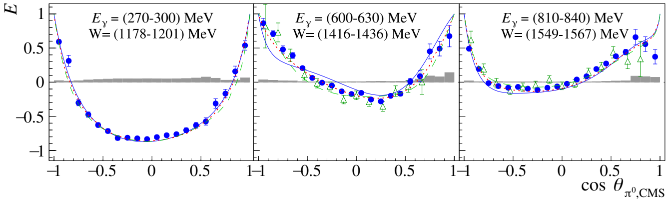

● F. Afzal et al., Phys.Rev.Lett. 132 (2024) 12, 121902

- Excellent agreement between A2 (diamond) and CBELSA/TAPS (amorphous)!
- Time and cost efficient measurement possible!

$\gamma p \to p\pi^0$: Dominant partial wave contributions (E (A2))

$$\check{E}(W, \cos\theta) = E(W, \cos\theta) \cdot \frac{d\sigma}{d\Omega}(W, \cos\theta) = \sum_{k=0}^{2L_{max}} (a_L(W))_k \cdot P_k^0(\cos\theta)$$

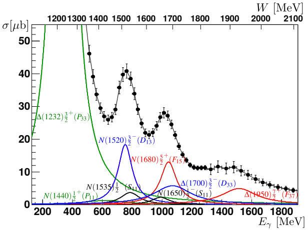

[Y. Wunderlich, F. Afzal et al., EPJA 53 (2017) 86]

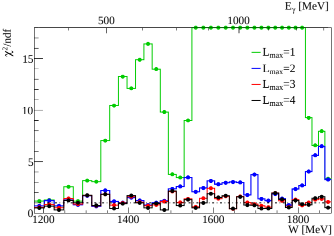

$\gamma p \to p\pi^0$: Dominant partial wave contributions (E (A2))

$$\check{E}(W, \cos\theta) = E(W, \cos\theta) \cdot \frac{d\sigma}{d\Omega}(W, \cos\theta) = \sum_{k=0}^{2L_{max}} (a_L(W))_k \cdot P_k^0(\cos\theta)$$

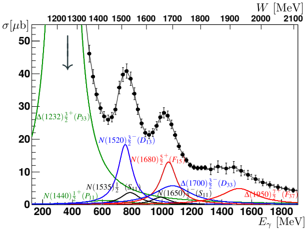

[Y. Wunderlich, F. Afzal et al., EPJA 53 (2017) 86]

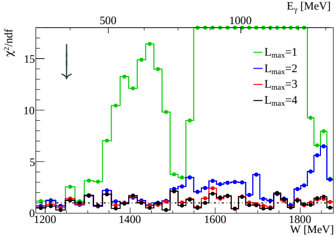

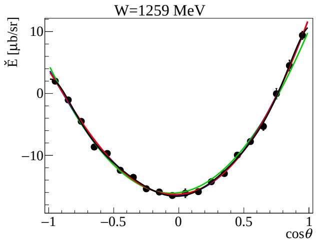

$\gamma p \rightarrow p\pi^0$: Dominant partial wave contributions (E (A2))

$$\check{E}(W, \cos\theta) = E(W, \cos\theta) \cdot \frac{d\sigma}{d\Omega}(W, \cos\theta) = \sum_{k=0}^{2L_{max}} (a_L(W))_k \cdot P_k^0(\cos\theta)$$

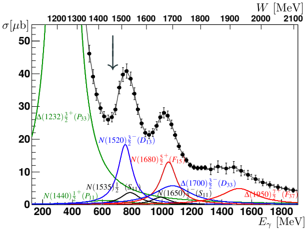

[Y. Wunderlich, F. Afzal et al., EPJA 53 (2017) 86]

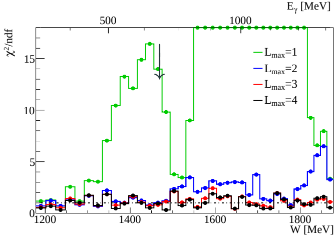

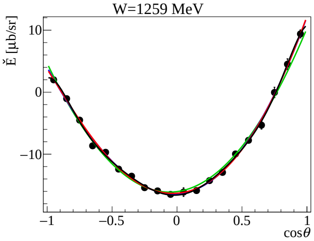

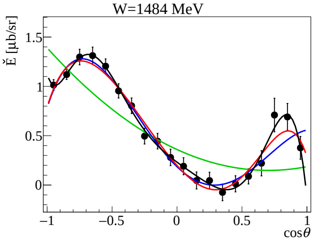

$\gamma p \to p\pi^0$: Dominant partial wave contributions (E (A2))

$$\check{E}(W, \cos\theta) = E(W, \cos\theta) \cdot \frac{d\sigma}{d\Omega}(W, \cos\theta) = \sum_{k=0}^{2L_{max}} (a_L(W))_k \cdot P_k^0(\cos\theta)$$

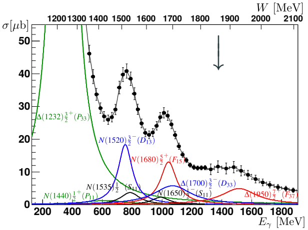

[Y. Wunderlich, F. Afzal et al., EPJA 53 (2017) 86]

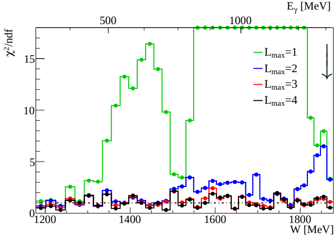

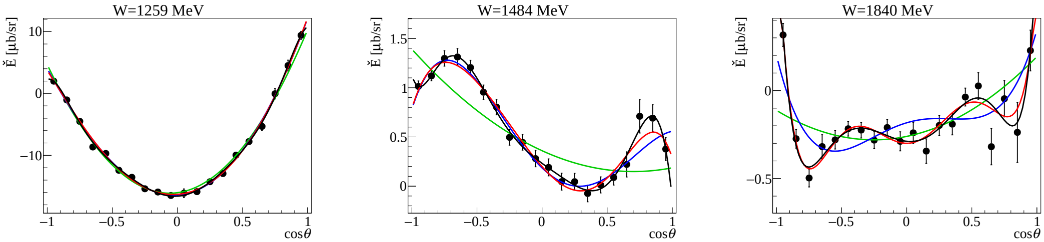

$\gamma p \to p\pi^0$: Dominant partial wave contributions (E (A2))

$$\check{E}(W,\cos\theta) = E(W,\cos\theta)\cdot\frac{d\sigma}{d\Omega}(W,\cos\theta) = \sum_{k=0}^{2L_{max}} (a_L(W))_k \cdot P_k^0(\cos\theta)$$

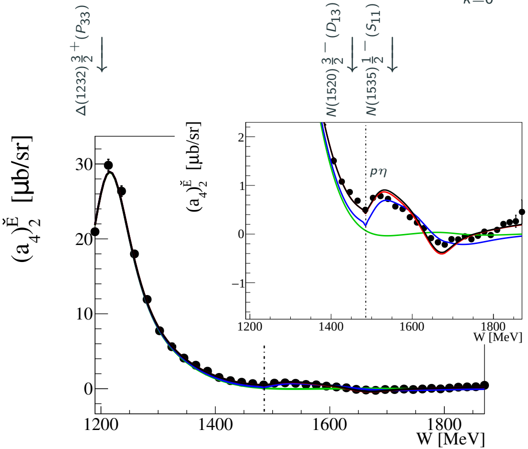

[F. Afzal et al., Phys.Rev.Lett. 132 (2024) 12, 121902]

$$(a_4)_2^{\check{E}} = \langle P,P\rangle$$ (green)

$$+\langle S,D\rangle + \langle D,D\rangle$$ (blue)

$$+\langle P,F\rangle + \langle F,F\rangle$$ (red)

$$+\langle D,G\rangle + \langle G,G\rangle$$ (black)

$p\eta$ cusp is well visible in the data and BnGa-2014-02 PWA ($< S, D >$).

$E2/M1$ ratio in the $N \to \Delta(1232)$ transition (A2)

UNIVERSITÄT BONN

- Measurement with MAMI - 450 MeV e^- beam; New precision data for $\gamma p \to \pi^0 p$
- Quantify deviation from a spherical shape for the nucleon and/or the $\Delta(1232)$ resonance
  $\to$ Measurement of the resonant quadrupole transition ($E2$) relative to the resonant dipole transition ($M1$)
- Helicity dependent cross section in the $\Delta(1232)$ region
  $\Delta\sigma = \sigma_{3/2} - \sigma_{1/2}$

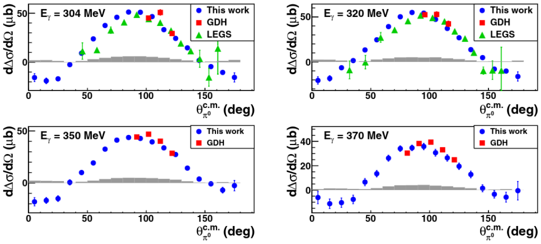

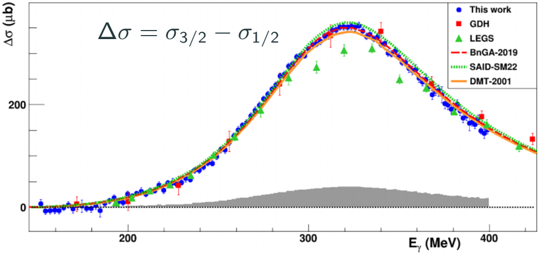

E. Mornacchi et al., Phys.Rev.C 109 (2024) 5, 055201

Legendre moment analysis truncating at $L_{max} = 1$ (S and P-wave):

$$(a_1)_0 \simeq -\mathrm{Im}[M_{1+}]^2 + 6\mathrm{Im}[E_{1+}]\mathrm{Im}[M_{1+}] \; ;$$
$$(a_1)_2 \simeq 2\mathrm{Im}[M_{1+}]^2 - 2\mathrm{Im}[M_{1-}]\mathrm{Im}[M_{1+}] \simeq 2\mathrm{Im}[M_{1+}]^2$$

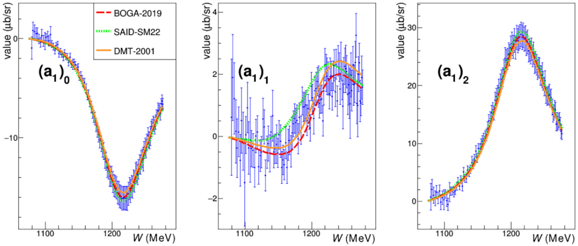

$$R_L = \frac{1}{3}\frac{(a_1)_0}{(a_1)_2} + \frac{1}{6} \simeq R_{EM}$$

$$R_{EM} = \frac{E2}{M1} \equiv \left.\frac{\mathrm{Im}[E^{3/2}_{1+}]}{\mathrm{Im}[M^{3/2}_{1+}]}\right|_{M_\Delta}$$

E. Mornacchi et al., Phys.Rev.C 109 (2024) 5, 055201

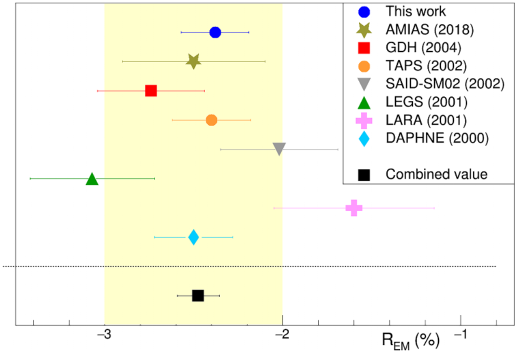

Measurements off protons ($\gamma p \to p\eta$)

$\gamma p \rightarrow p\eta$: Measurement of cross sections (A2)

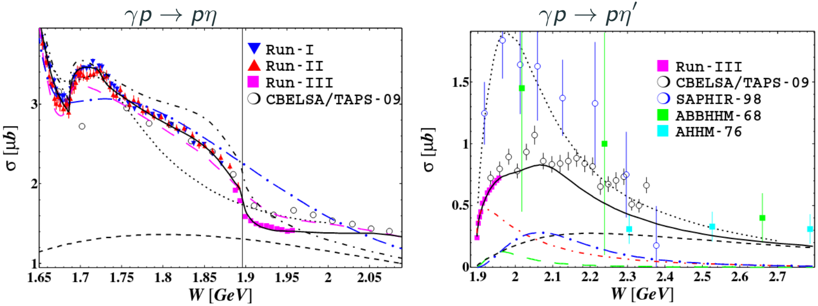

V.L. Kashevarov et al., Phys. Rev. Lett. 118, 21 (2017), p. 212001

- key role for description: 3 $S-$wave resonances: $N(1535)\frac{1}{2}^-$, $N(1650)\frac{1}{2}^-$ and $N(1895)\frac{1}{2}^-$
- strong $p\eta'$ cusp observed in $p\eta$ cross section
- $N(1895)\frac{1}{2}^-$ needed for description of $p\eta'$ cusp and fast rise of $p\eta'$ cross section

$\gamma p \to p\eta$: Precise beam asymmetry Σ data (CBELSA/TAPS)

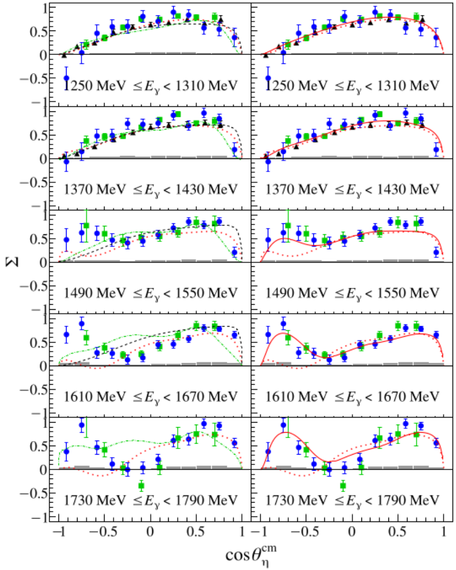

[F. Afzal et al., Phys. Rev. Lett. 125, 152002 (2020)]

- ● CBELSA/TAPS data (F. Afzal et al.)
- ▲ GRAAL data (O. Bartalini et al., Eur. Phys. J. A33 (2007) 169)
- ■ CLAS data (P. Collins et al., Phys. Lett. B 771 (2017) 213-221)

BnGa-2014-02   JüBo-2015-FitB ηMAID

BnGa-2019

$\gamma p \rightarrow p\eta$: Precise beam asymmetry Σ data (CBELSA/TAPS)

UNIVERSITÄT BONN

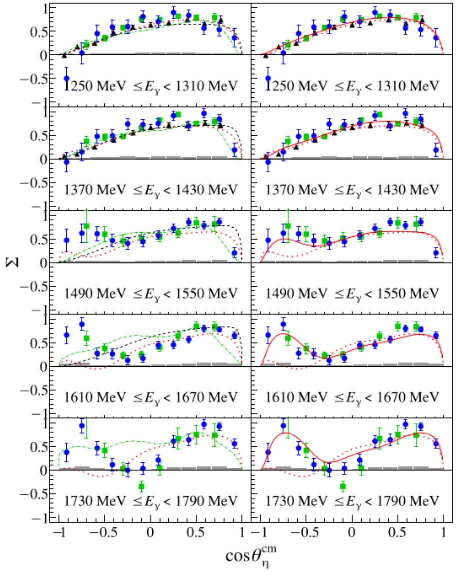

[F. Afzal et al., Phys. Rev. Lett. 125, 152002 (2020)]

- ● CBELSA/TAPS data (F. Afzal et al.)
- ▲ GRAAL data (O. Bartalini et al., Eur. Phys. J. A33 (2007) 169)
- ■ CLAS data (P. Collins et al., Phys. Lett. B 771 (2017) 213-221)

BnGa-2014-02   JüBo-2015-FitB ηMAID

BnGa-2019

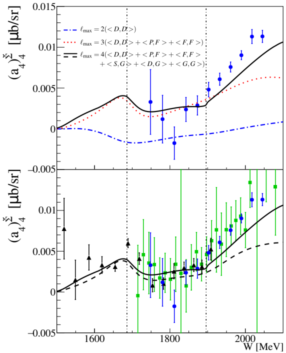

High angular coverage

Sensitivity to $< S, G >$ interference

$p\eta'$ cusp effect visible in Legendre coefficient!

Further confirmation of $N(1895)\frac{1}{2}^-$!

$N^* \to p\eta$ branching ratios (CBELSA/TAPS)

Combined analysis of the polarization observables σ, G, E, T, P, H in $\gamma p \to p\eta$

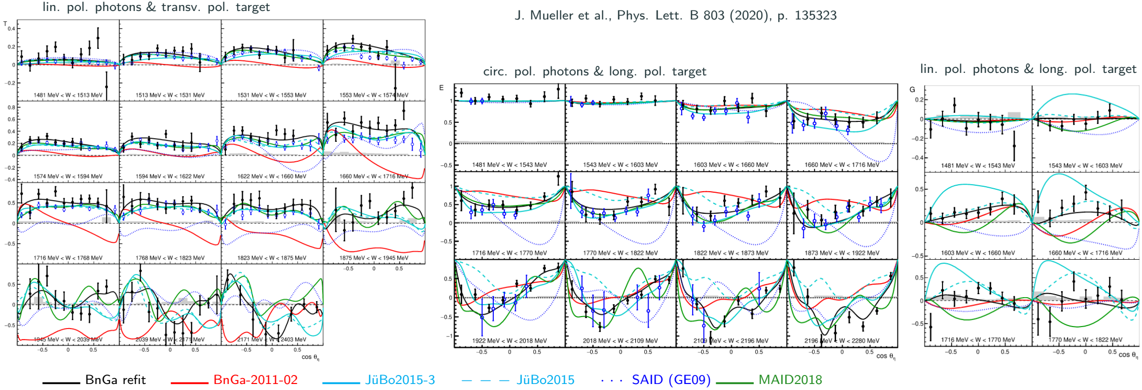

	$N(1535)\frac{1}{2}^-$	$N(1650)\frac{1}{2}^-$
BnGa refit	0.41 ± 0.04	0.33 ± 0.04
PDG 2017	$0.32 - 0.52$	$0.14 - 0.22$

Large and heavily discussed difference in the $p\eta$-branching ratio of $N(1535)\frac{1}{2}^-$ and $N(1650)\frac{1}{2}^-$ now significantly reduced!

Measurements off neutrons

Measurements off neutrons

- Motivation:
  - Electromagnetic excitation is isospin dependent
  - Measurements off neutrons are essential for an isospin separation
  - Different resonance contributions possible
- Experimentally complicated to measure:
  - No free neutrons → helium, deuterium, deuterated butanol targets
  - Nuclear Fermi motion and FSI effects make interpretation of results difficult
  - Low detection efficiency of neutrons

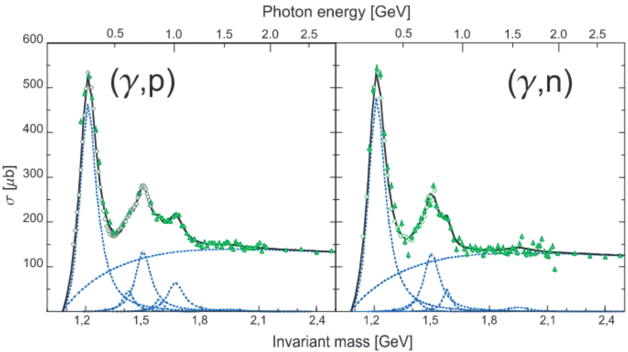

[B. Krusche, J.Phys.Conf.Ser. 349 (2012) 012003]

narrow peak observed in $\gamma n \to n\eta$
at $W = (1670 \pm 5)$ MeV with $\Gamma = 30$ MeV

[D. Werthmüller et al., Phys.Rev. C90 (2014) no.1, 015205]

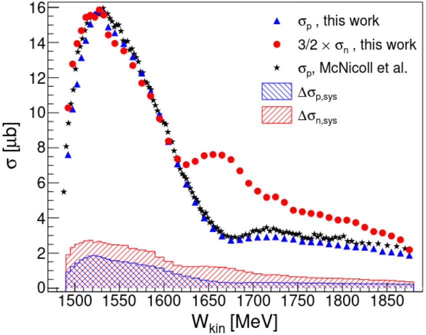

$\gamma n \to n\eta$: Narrow structure in σ, E (A2)

narrow peak observed in $\gamma n \to n\eta$
at $W = (1670 \pm 5)$ MeV with $\Gamma = 30$ MeV

[D. Werthmüller et al., Phys.Rev. C90 (2014) no.1, 015205]

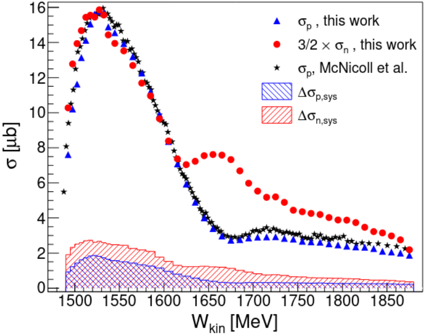

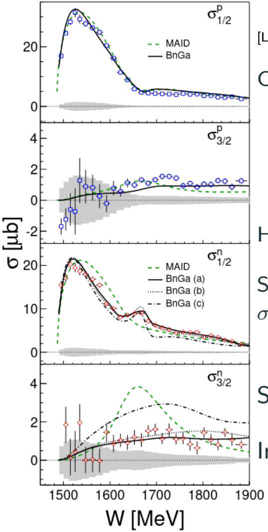

[L. Witthauer et al., Phys. Rev. Lett. 117, no. 13, 132502 (2016)]

Circularly pol. photons & long. pol. target

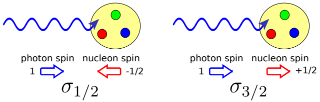

Helicity asymmetry: $E = \frac{\sigma_{1/2} - \sigma_{3/2}}{\sigma_{1/2} + \sigma_{3/2}}$

Spin dependent cross sections
$\sigma_{1/2(3/2)} = \sigma_0 \cdot (1 \pm E)$

Structure only present in $\sigma^n_{1/2}$!

Intrinsic resonance/ interference effects?

$\gamma n \to n\eta$: Results of T, P, H (CBELSA/TAPS)

UNIVERSITÄT BONN

- More data taken for T, P, H with coherent edges at 1300 MeV, 1600 MeV
- Ongoing analyses of different final states ($N\pi^0$, $N\eta$, $N\eta'$, $N\omega$, $N\pi^0\pi^0$, $N\pi^0\eta$...) and PWA of the data

$\gamma d \to \eta n(p)$

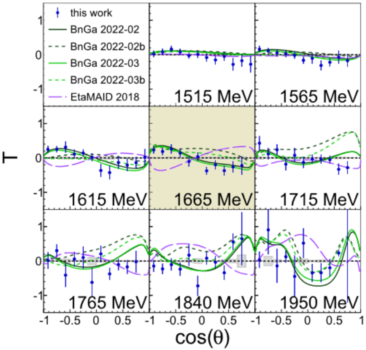

[N. Jermann et al., Eur.Phys.J.A 59 (2023) 10, 232]

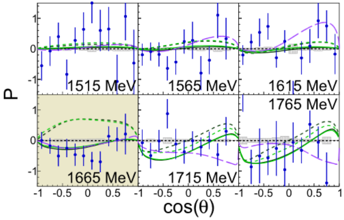

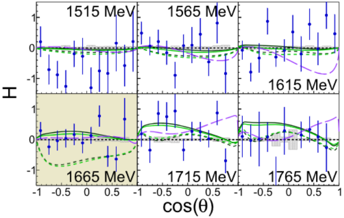

— BnGa 2022-02, — BnGa 2022-03: interference effect: $S_{11}(1535)\frac{1}{2}^-$ and $S_{11}(1650)\frac{1}{2}^-$

- - - BnGa 2022-02 b, - - - BnGa 2022-03 b: new narrow resonance in P_{11}-wave: $P_{11}(1680)\frac{1}{2}^+$

- - - EtaMAID 2018: interference effect: $S_{11}(1535)\frac{1}{2}^-$ and $P_{11}(1710)\frac{1}{2}^+$

$\rightarrow$ data favors $S - S$ wave interference

Impact of data

Impact of photoproduction data - Updates in PDG 2020

UNIVERSITÄT BONN

Particle	J^P	overall	PWA	$N\gamma$	$N\pi$	$\Delta\pi$	$N\sigma$	$N\eta$	ΛK	ΣK	$N\rho$	$N\omega$	$N\eta'$
N	$1/2^+$	****											
$N(1440)$	$1/2^+$	****	$\circ$ $\diamond_g$ $\star$ $\triangleright$	****	****	****	***	-			-		
$N(1520)$	$3/2^-$	****	$\circ$ $\diamond$ $\star$ $\triangleright$	****	****	****	**	****			- - - -		
$N(1535)$	$1/2^-$	****	$\circ$ $\diamond$ $\star$ $\triangleright$	****	****	***	*	****			- -		
$N(1650)$	$1/2^-$	****	$\circ$ $\diamond$ $\star$ $\triangleright$	****	****	***	*	****	*- -	- -	- -		
$N(1675)$	$5/2^-$	****	$\circ$ $\diamond$ $\star$ $\triangleright$	****	****	****	***	*	*	*	-		
$N(1680)$	$5/2^+$	****	$\circ$ $\diamond$ $\star$ $\triangleright$	****	****	****	***	*	*	*	- - - -		
$N(1700)$	$3/2^-$	***	$\circ$ $\triangleright$	**	***	***	*	*	- -	-	-		
$N(1710)$	$1/2^+$	****	$\circ$ $\diamond$ $\triangleright$	****	****	*-		***	**	*	*	*	
$N(1720)$	$3/2^+$	****	$\circ$ $\diamond$ $\star$ $\triangleright$	****	****	***	*	*	****	*	*-	*	
$N(1860)$	$5/2^+$	**	$\triangleright$	*	**		*	*					
$N(1875)$	$3/2^-$	***	$\circ$ $\triangleright$	**	**	*	**	*	*	*	*	*	
$N(1880)$	$1/2^+$	***	$\circ$ $\triangleright$	**	*	**	*	*	**	**		**	
$N(1895)$	$1/2^-$	****	$\circ$ $\triangleright$	****	*	*	*	****	**	**	*	*	****
$N(1900)$	$3/2^+$	****	$\circ$ $\diamond$ $\triangleright$	****	**	**	*	*	**	**	-	*	**
$N(1990)$	$7/2^+$	**	$\circ$ $\diamond$ $\triangleright$	**	**			*	*	*			
$N(2000)$	$5/2^+$	**	$\circ$ $\star$	**	*-	**	*	*	-	-	- -	*	
$N(2040)$	$3/2^+$	*	$\triangleright$		*								
$N(2060)$	$5/2^-$	***	$\circ$ $\diamond_g$ $\triangleright$	***	**	*	*	*	*	*	*	*	
$N(2100)$	$1/2^+$	***	$\circ$ $\triangleright$	**	***	**	**	*	*		*	*	**
$N(2120)$	$3/2^-$	***	$\circ$ $\triangleright$	***	**	**	**		**	*		*	*
$N(2190)$	$7/2^-$	****	$\circ$ $\diamond$ $\star$ $\triangleright$	****	****	****	**	*	**	*	*	*	
$N(2220)$	$9/2^+$	****	$\circ$ $\diamond$ $\star$	**	****			*	*	*			
$N(2250)$	$9/2^-$	****	$\circ$ $\diamond$ $\star$ $\triangleright$	**	****			*	*	*			
$N(2300)$	$1/2^+$	**			**								
$N(2570)$	$5/2^-$	**			**								
$N(2600)$	$11/2^-$	***	$\star$		***								
$N(2700)$	$13/2^+$	**			**								

- Until 2010: almost only results from πN scattering used in the PDG
- PWA groups:
  $\circ$ BnGa-2019, $\diamond$ JüBo-2017, $\star$ SAID-MA19, $\triangleright$ KSU model include photoproduction data with different final states from several experiments
- Now: new values from the fits are entering the PDG!

[A. Thiel, F. Afzal, Y. Wunderlich, Prog. Part. Nucl. Phys. 125 (2022) 103949]

Summary

- Light baryon spectroscopy is experimentally challenging
  $\rightarrow$ Need to measure several polarization observables with large energy and angular coverage!
- High precision data measured at the A2 and CBELSA/TAPS experiments for many different final states
  $\rightarrow$ Sensitivity up to G-waves reached! $p\eta$ and $p\eta'$ cusps observed in pol. observables!
  $\rightarrow$ Significant contributions to confirming poorly known states like $N(1895)\frac{1}{2}^-$
  $\rightarrow$ Better understanding of narrow structure in $n\eta$ (S-S wave interference)
- Our knowledge of the spectrum and the properties of baryons is steadily increasing!

- More polarization observables data for photoproduction off the neutron for different final states
- Investigation of strange baryons: KY-photoproduction data - new experiment planned at ELSA

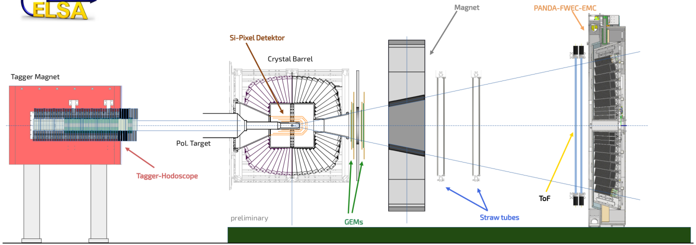

Backup Slides

Measurements off neutrons - cross section data for $\gamma d \to \pi^0 n(p)$ (A2)

- Complicated to measure due to no free neutrons → helium, deuterium, deuterated butanol targets
- Nuclear Fermi motion effects eliminated by a complete kinematic reconstruction of the final state
- FSI estimated through comparison of quasi-free and free proton data

○ quasi-free proton △ quasi-free neutron ▲ free neutron

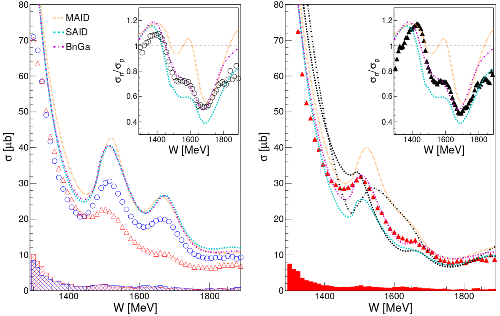

[M. Dieterle et al., Phys. Rev. Lett. 112.14 (2014), p. 142001]
[M. Dieterle et al., Phys. Rev. C (2018), pp. 065205-1-065205-28]

Significant FSI effects in quasi-free proton data

→ FSI effects corrected assuming FSI effect is equal for participant protons and neutrons!

Measurements off neutrons - cross section data for $\gamma d \rightarrow \pi^0 n(p)$ (A2)

- Complicated to measure due to no free neutrons $\rightarrow$ helium, deuterium, deuterated butanol targets
- Nuclear Fermi motion effects eliminated by a complete kinematic reconstruction of the final state
- FSI estimated through comparison of quasi-free and free proton data

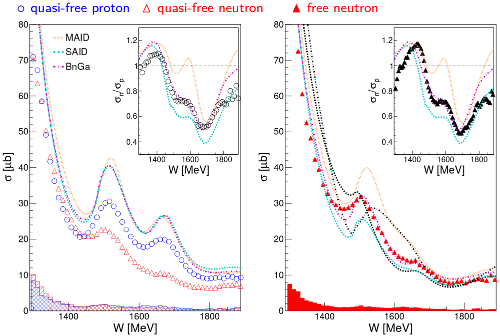

[M. Dieterle et al., Phys. Rev. Lett. 112.14 (2014), p. 142001]
[M. Dieterle et al., Phys. Rev. C (2018), pp. 065205-1-065205-28]

Significant FSI effects in quasi-free proton data

$\rightarrow$ FSI effects corrected assuming FSI effect is equal for participant protons and neutrons!

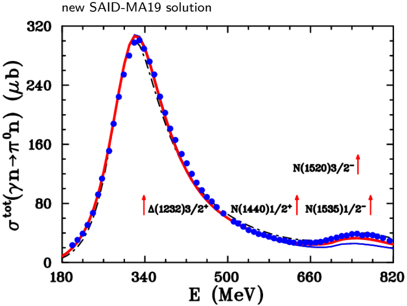

[W.J. Briscoe, Phys.Rev.C 100 (2019) 6, 065205]

$\rightarrow$ Photon decay amplitudes $A_{3/2}(n)$ and $A_{1/2}(n)$ for $N^* \rightarrow \gamma n$ extracted

Impact of polarization observables in $\gamma p \to p\pi^0$

- The variance of all the three PWAs (JüBo, SAID, BnGa) summed over all $\gamma p \to p\pi^0$ multipoles up to $L = 4$
- Variance between the different PWAs decreases!

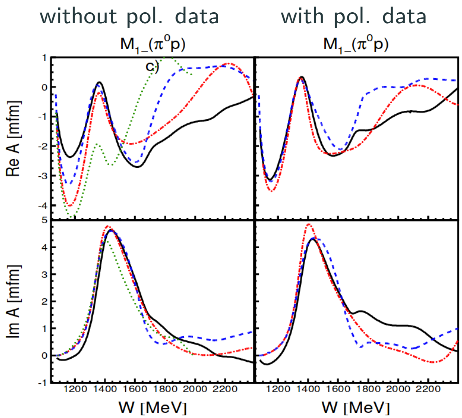

[Anisovich et al., Eur.Phys.J. A52 (2016) no.9, 284]

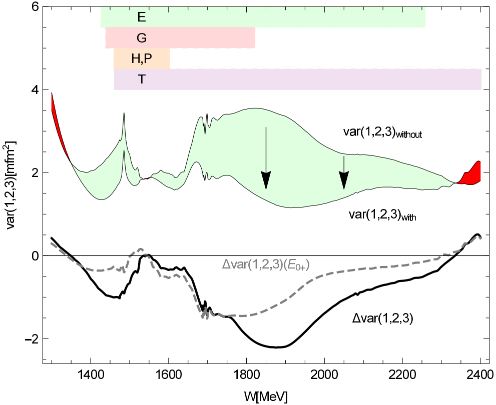

$SU(6) x O(3)$ supermultiplets

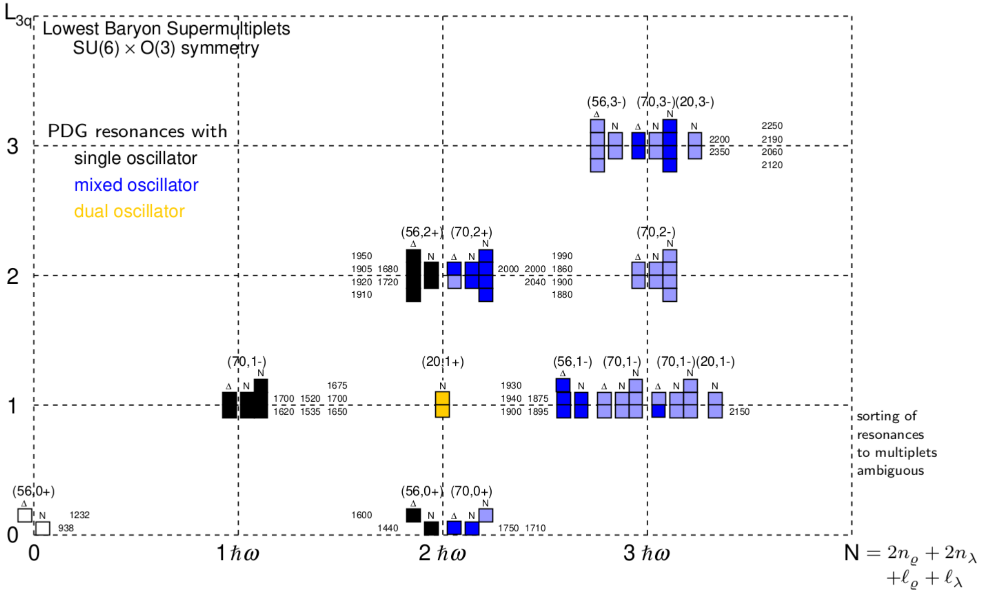

$\gamma p \to p\pi^0\pi^0$: Importance of cascade decays

- Multi-meson final states like $p\pi^0\pi^0$ are preferred at higher energies
- Less background amplitudes than $p\pi^+\pi^-$ but cannot discriminate between N^*/Δ^*
- Access to sequential decays

$\to$ talk by P. Mahlberg [HK 57.1, Thursday, 14:00]

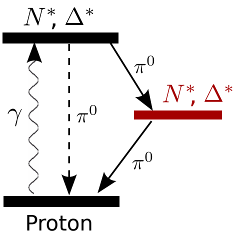

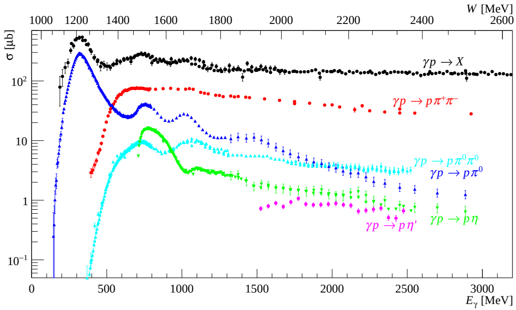

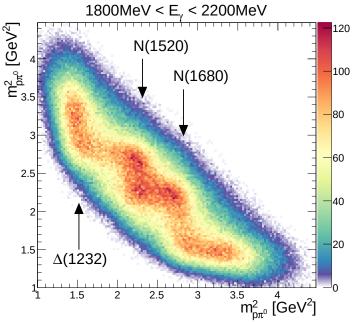

Polarization observables in $p\pi^0\pi^0$ - 4D extraction

Data analyzed in full 3 body kinematics

[T. Seifen et al., arXiv:2207.01981v1 [nucl-ex]]

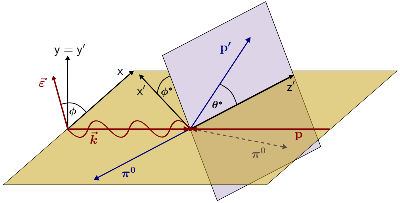

5 kinematic variables:
$E_\gamma, \cos\vartheta_{\pi^0}, m_{p\pi^0}, \phi^*_{p\pi^0}, \theta^*_{p\pi^0}$

More pol. observables accessible

Photon Pol.		Target Pol. Axis		
		x	y	z
unpolarised	σ	P_x	P_y	P_z
linear $\sin(2\phi)$	I^s	P_x^s	P_y^s	P_z^s
linear $\cos(2\phi)$	I^c	P_x^c	P_y^c	P_z^c
circular	$I^\odot$	$P_x^\odot$	$P_y^\odot$	$P_z^\odot$

Polarization observables in $p\pi^0\pi^0$ - 4D extraction

Data analyzed in full 3 body kinematics

[T. Seifen et al., arXiv:2207.01981v1 [nucl-ex]]

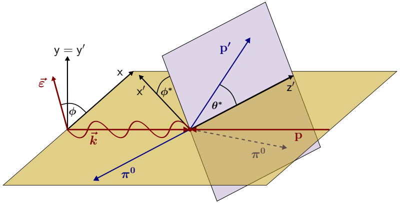

5 kinematic variables:

$E_\gamma, \cos\vartheta_{\pi^0}, m_{p\pi^0}, \phi^*_{p\pi^0}, \theta^*_{p\pi^0}$

More pol. observables accessible

Photon Pol.		Target Pol. Axis		
		x	y	z
unpolarised	σ	P_x	P_y	P_z
linear $\sin(2\phi)$	I^s	P_x^s	P_y^s	P_z^s
linear $\cos(2\phi)$	I^c	P_x^c	P_y^c	P_z^c
circular	$I^\odot$	$P_x^\odot$	$P_y^\odot$	$P_z^\odot$

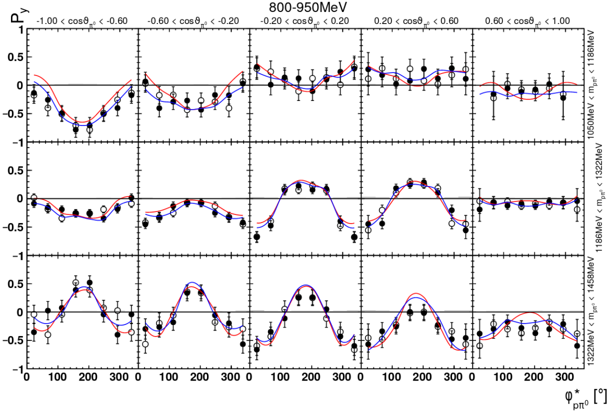

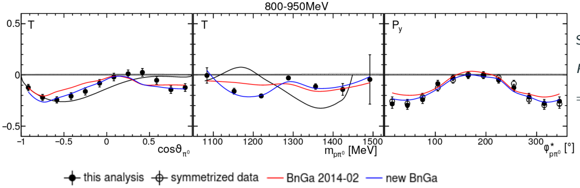

Symmetry:

$P_y(2\pi - \phi^*)$

$= +P_y(\phi^*)$

Polarization observables in $p\pi^0\pi^0$ - New branching ratios

4th resonance region:

	$\Delta(1910)\,\frac{1}{2}^+$, $\Delta(1920)\,\frac{3}{2}^+$, $\Delta(1905)\,\frac{5}{2}^+$, $\Delta(1950)\,\frac{7}{2}^+$ Δ^*, $S=\frac{3}{2}$, $L=2$, ϕ^S_{space}	$N(1880)\,\frac{1}{2}^+$, $N(1900)\,\frac{3}{2}^+$, $N(2000)\,\frac{5}{2}^+$, $N(1990)\,\frac{7}{2}^+$ N^*, $S=\frac{3}{2}$, $L=2$, $\phi^{MS}_{\text{space}}+\phi^{MA}_{\text{space}}$
BR into ground state $N(938)\pi$ or $\Delta(1232)\pi$	$(44\pm7)\%$	$(34\pm6)\%$
BR into excited states (L=1) $N(1520)\pi$, $N(1535)\pi$, $N\sigma$	$(5\pm2)\%$	$(21\pm5)\%$

Polarization observables in $p\pi^0\pi^0$ - New branching ratios

4th resonance region:

	$\Delta(1910)\frac{1}{2}^+$, $\Delta(1920)\frac{3}{2}^+$, $\Delta(1905)\frac{5}{2}^+$, $\Delta(1950)\frac{7}{2}^+$ Δ^*, $S=\frac{3}{2}$, $L=2$, ϕ^S_{space}	$N(1880)\frac{1}{2}^+$, $N(1900)\frac{3}{2}^+$, $N(2000)\frac{5}{2}^+$, $N(1990)\frac{7}{2}^+$ N^*, $S=\frac{3}{2}$, $L=2$, $\phi^{MS}_{\text{space}}+\phi^{MA}_{\text{space}}$
BR into ground state $N(938)\pi$ or $\Delta(1232)\pi$	$(44\pm7)\%$	$(34\pm6)\%$
BR into excited states (L=1) $N(1520)\pi$, $N(1535)\pi$, $N\sigma$	$(5\pm2)\%$	$(21\pm5)\%$

[A. Thiel et al., Phys. Rev. Lett. 114, 091803]

Harmonic oscillator model (orbital excitation L=2)

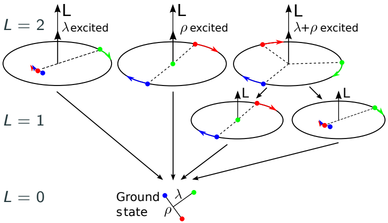

Polarization observables in $p\pi^0\pi^0$ - New branching ratios

4th resonance region:

	$\Delta(1910)\frac{1}{2}^+, \Delta(1920)\frac{3}{2}^+, \Delta(1905)\frac{5}{2}^+, \Delta(1950)\frac{7}{2}^+$ $\Delta^*,\ S = \frac{3}{2},\ L = 2,\ \phi^S_{\text{space}}$	$N(1880)\frac{1}{2}^+, N(1900)\frac{3}{2}^+, N(2000)\frac{5}{2}^+, N(1990)\frac{7}{2}^+$ $N^*,\ S = \frac{3}{2},\ L = 2,\ \phi^{MS}_{\text{space}} + \phi^{MA}_{\text{space}}$
BR into ground state $N(938)\pi$ or $\Delta(1232)\pi$	$(44 \pm 7)\%$	$(34 \pm 6)\%$
BR into excited states (L=1) $N(1520)\pi$, $N(1535)\pi$, $N\sigma$	$(5 \pm 2)\%$	$(21 \pm 5)\%$

→ talk by P. Mahlberg [HK 57.1, Thursday, 14:00]

[A. Thiel et al., Phys. Rev. Lett. 114, 091803]

Harmonic oscillator model (orbital excitation L=2)

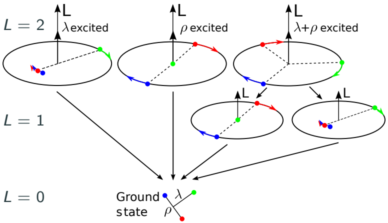

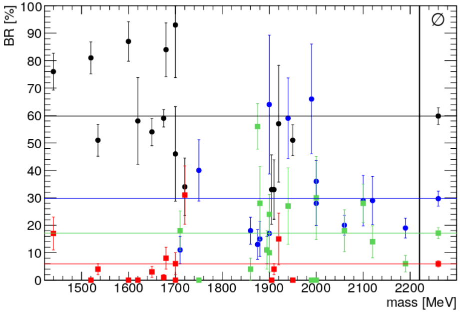

One-oscillator excitations decay into the ground states

One-oscillator excitations decay into excited states

Mixed-oscillator excitations decay into the ground states

Mixed-oscillator excitations decay into excited states

[T. Seifen et al., arXiv:2207.01981v1 [nucl-ex]]